Hydrology and Earth System Sciences Discussions

Dissolved inorganic carbon export from carbonate and silicate catchments estimated from carbonate chemistry and $\delta^{13}C_{DIC}$

W. J. Shin[1,2], G. S. Chung[1], D. Lee[3], and K. S. Lee[2,4]

[1]Department of Geology and Earth Environmental Sciences, Chungnam National University, Daejeon 305-764, Republic of Korea
[2]Division of Earth and Environmental Science, Korea Basic Science Institute, Daejeon 305-333, Republic of Korea
[3]Korea Research Institute of Standards and Science, Daejeon 305-340, Republic of Korea
[4]Graduate School of Analytical Science and Technology, Chungnam National University, Daejeon 305-764, Republic of Korea

Title Page

Abstract | Introduction

Conclusions | References

Tables | Figures

◄ | ►

◄ | ►

Back | Close

Full Screen / Esc

Printer-friendly Version

Interactive Discussion

Dissolved inorganic carbon export from carbonate and silicate

W. J. Shin et al.

Title Page

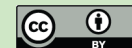| Abstract | Introduction |
| Conclusions | References |
| Tables | Figures |

Back | Close

Full Screen / Esc

Printer-friendly Version

Interactive Discussion

Abstract

We investigated dissolved inorganic carbon (DIC) exchange associated with groundwater discharge and stream flow from two upstream catchments with distinct basement lithology (silicate vs. carbonate). The effects of catchment lithology were evident in the spring waters showing lower $\delta^{13}C_{DIC}$ and alkalinity (-16.2 ± 2.7‰ and 0.09 ± 0.03 meq L^{-1}, respectively) in the silicate and higher values (-9.7 ± 1.5‰ and 2.0 ± 0.2 meq L^{-1}) in the carbonate catchment. The streams exhibited relatively high $\delta^{13}C_{DIC}$ values, -6.9 ± 1.6‰ and -7.8 ± 1.5‰, in silicate and carbonate catchments, respectively, indicating CO_2 degassing during groundwater discharge and stream flow. The catchment lithology affected the pattern of DIC export. The CO_2 degassing from stream and groundwater could be responsible for 8–55% of the total DIC export in the silicate catchment, whereas the proportion is comparatively low (0.4–5.6%) in the carbonate catchment. We emphasize the importance of dynamic carbon exchange occurring at headwater regions and its variability with catchment lithology for a more reliable carbon budget in river systems.

1 Introduction

The current increase of atmospheric carbon dioxide, a greenhouse gas, and associated climate changes necessitate a more in-depth understanding of the global carbon cycle (Friedlingstein et al., 2003; Govindasamy et al., 2005). Rivers play an important role in global carbon cycling by transporting carbon from terrestrial to marine realms. The global flux of carbon transported by rivers in the form of dissolved inorganic carbon (DIC) is estimated to be 0.43×10^{15} g C yr^{-1}, representing about 40% of the total global carbon flux (Meybeck, 1987). Moreover, the evasion of CO_2 from rivers during DIC transport is an important component of the atmospheric CO_2 budget (Richey et al., 2002). Thus, considerable effort has been directed toward quantifying both vertical (evasion of CO_2) and lateral (discharge) exports of DIC via rivers (Dubois et al., 2010).

In upstream regions (e.g., headwater catchments) where the stream flow is mainly due to groundwater discharge, groundwater acts as a conduit of subsurface DIC transport across the interface between terrestrial (e.g., soils) and aquatic reservoirs (e.g., streams). The onset of carbon exchange at the headwater regions is characterized by enhanced CO_2 evasion due to strong CO_2 over-saturation of the groundwater. Because the effect of groundwater DIC is transient and is only observed near the immediate source at the first order stream, carbon exchange at this interface has been largely unexplored (Johnson et al., 2008; Öquist et al., 2009). Therefore, a more quantitative understanding of carbon exchange in headwater systems is essential to derive a reliable carbon budget of river systems.

An isotope tracer, $\delta^{13}C_{DIC}$, is especially useful because it reveals reaction pathways and transport processes that may otherwise be difficult to discern with normative carbonate systems (Tan and Edmond, 1993; Taylor and Fox, 1996; Yang et al., 1996). The DIC in river water originates from several sources, including influx of soil CO_2 via groundwater, CO_2 exchange with the atmosphere, in-river respiration, and dissolution of carbonate rocks. About 67% of the DIC in the world's rivers is known to originate from soil CO_2 (Meybeck, 1987; Ludwig et al., 1997). Based on stoichiometric considerations, the proportion of soil CO_2 in rivers ranges from ~50% in carbonate catchments (another 50% is from the carbonate minerals) to ~100% in silicate catchments. In upstream regions where groundwater contributes largely to stream flow, the input of groundwater containing DIC from soil CO_2 lowers the $^{13}C/^{12}C$ ratio of DIC in river water because soil CO_2 is largely derived from the microbial degradation of soil organic matter (Amiotte-Suchet et al., 1999; Finlay, 2003). In contrast, atmospheric exchange and dissolution of carbonate minerals increase the $^{13}C/^{12}C$ ratio of DIC because these sources are enriched in ^{13}C relative to ^{12}C (Amiotte-Suchet et al., 1999). In addition to the strong over-saturation with CO_2 in groundwater components, stream water in upstream regions may also be more turbulent, causing rapid degassing of CO_2 into the atmosphere and remarkable ^{13}C enrichment in DIC (Doctor et al., 2007).

Dissolved inorganic carbon export from carbonate and silicate

W. J. Shin et al.

The uppermost tributaries of the South Han River (SHR), South Korea, provide an ideal hydro-geological setting to investigate factors controlling $\delta^{13}C_{DIC}$ and carbonate chemistry because they drain catchments with contrasting bedrock lithologies: silicate vs. carbonate. Moreover, their drainage system that consists of the first to fifth order streams provides an adequate condition for studies on carbon exchanges from the headwater regions to the main channels. In this study, we measured the stable carbon isotopic composition of DIC and carbonate chemistry from springs and streams draining upstream catchments with silicate and carbonate basements. The objectives were to (1) determine factors controlling carbonate chemistry and $\delta^{13}C_{DIC}$ in catchments with different lithologies and (2) quantify lateral and vertical transport of DIC at upstream catchments and their possible variation with the catchment lithology.

2 Materials and methods

2.1 Description of the study sites

The study sites were two upstream tributaries of the SHR in the middle part of the Korean peninsula (Fig. 1). Both catchments are located at the headwater regions of the SHR basin. The Odae drains a basin (452 km^2) dominated exclusively by silicate rocks, consisting of Precambrian metamorphic crystalline rock, Permian to Triassic sandstone and shale, and Jurassic to Cretaceous granite. In contrast, the Jijang drains a basin (225 km^2) dominated by Cambro-Ordovician carbonate rock with some sandstone at its upper reach. The elevation of the study sites ranges from 340 to 1560 m for the Odae and from 260 to 1570 m for the Jijang catchment.

The vegetation in the study area consisted largely of C$_3$ plants (mixed deciduous broadleaf and conifer forests) with seasonally cultivated C$_4$ (e.g., corn) crops. Table 1 presents information on the two streams (Water Management Information System: www.wamis.go.kr).

2.2 Sampling and analytical procedures

Water sampling and in-situ measurements of geochemical parameters were conducted at four locations on a biweekly basis for 18 months (July 2004 to December 2005). Water was collected from the two perennial springs and the outlet of the main channel (fifth-order stream) in both catchments. In the silicate catchment (Odae), we chose a perennial spring located at the bottom of a sandstone cliff from which water was discharging at $\sim$37 m^3 day^{-1}. In the carbonate catchment (Jijang), we also chose a perennial spring flowing from the base of a carbonate cliff. Although sampling began in July 2004, this study focused on the data from 2005 because a more complete dataset was available in terms of measured parameters and seasonal coverage.

Temperature, pH, dissolved oxygen (DO), and electrical conductivity (EC) were measured on site during water sampling using a YK-2001PH portable meter. Alkalinity was measured by titration with 0.05N HCl according to the Gran method (Rounds and Wilde, 2001). To fully characterize the carbonate system, ion activities were evaluated by PHREEQC (Parkhurst and Appelo, 1999). The partial pressure of CO_2 (pCO_2) was calculated by the speciation outputs from PHREEQC. The temperature-dependent equilibrium constants for the three species (H_2CO_3, HCO_3^-, and CO_3^{2-}) of the DIC summarized by Langmuir (1997) were used to calculate the activities of the three species.

For $\delta^{13}C_{DIC}$ analysis, water samples were collected using two evacuated glass bottles (150 mL) pre-loaded with 85% phosphoric acid and a magnetic stir bar, as reported by Atekwana and Krishnamurthy (1998). Water sampling was carried out in the field using a syringe with a 0.45-μm Millipore membrane filter. Samples were stored in a refrigerator prior to analysis. The DIC in water samples was converted into CO_2 gas by a gas-evolution technique (Atekwana and Krishnamuthy, 1998). The CO_2 gas was then extracted and cryogenically purified. Next, the $\delta^{13}C$ values of the evolved CO_2 were measured using an Optima isotope-ratio mass spectrometer (GV Instruments, UK) at Chungnam National University. Carbon isotopic ratios are reported using standard δ notation, in per mil (‰) differences relative to the Vienna Pee Dee belemnite (VPDB)

standard, i.e., $\delta\,(‰) = (R_{\text{sample}} / R_{\text{standard}} - 1) \times 1000$, where R represents $^{13}C/^{12}C$. The analytical reproducibility was ±0.2‰.

3 Results

3.1 Spring waters

Figure 2 shows the precipitation, $\delta^{13}C_{\text{DIC}}$ values, and pCO_2 of the four water types. Ranges and averages of the measured parameters are shown in Table 2. The pH values in silicate and carbonate springs were between 5.1 and 6.9 (average of 6.1, $n = 23$) and between 7.7 and 8.5 (average of 8.0, $n = 23$), respectively. Alkalinities were between 0.05 and 0.17 meq L^{-1} (average of 0.09 meq L^{-1}) in the silicate spring and between 1.50 and 2.21 meq L^{-1} (average of 1.96 meq L^{-1}) in the carbonate spring. Figure 2b shows seasonal variations in $\delta^{13}C_{\text{DIC}}$ values of the spring waters. The silicate spring had $\delta^{13}C_{\text{DIC}}$ values ranging from −21.2 to −13.1‰ (average of −16.2 ± 2.7‰), and the carbonate spring had values from −13.2 to −8.1‰ (average of −9.7 ± 1.5‰). The pCO_2 showed contrasting values between silicate and carbonate waters (Fig. 2c). The silicate spring waters had pCO_2 values ranging from 827 to 42,546 ppmv (average of 7520 ppmv), and the carbonate spring waters had pCO_2 values from 372 to 2196 ppmv (average of 1245 ppmv).

The $\delta^{13}C_{\text{DIC}}$, alkalinity, and pH were the major parameters used to distinguish water derived from silicate and carbonate catchments. The two spring waters were distinguished by a pH of 7, and the silicate spring had a wider range than the carbonate spring (Fig. 3). The carbonate spring water had greater alkalinity with larger variability, whereas the variability of the silicate spring was limited.

3.2 Stream waters

The pH ranged from 6.8 to 8.1 (average of 7.6, $n = 15$) in the silicate stream and from 7.9 to 9.1 (average of 8.5, $n = 15$) in the carbonate stream. EC (from 11 to 122 $\mu S\,cm^{-1}$, average of 64, $n = 20$) and alkalinity (from 0.22 to 0.74 $meq\,L^{-1}$, aver-
5 age of 0.44, $n = 23$) were lower in the silicate stream than in the carbonate stream, where EC ranged from 222 to 433 $\mu S\,cm^{-1}$ (average of 301, $n = 19$), and alkalinity ranged from 1.18 to 1.83 $meq\,L^{-1}$ (average of 1.46, $n = 23$). As shown in Fig. 2b, the silicate stream had $\delta^{13}C_{DIC}$ values from -10 to -3.6‰, with an average of -6.9 ± 1.6‰ ($n = 23$), whereas values from the carbonate stream ranged from -11.2 to -6.1‰, with
10 an average of -7.8 ± 1.5‰ ($n = 23$). The pCO_2 was higher in the silicate stream, rang-ing from 150 to 3380 ppmv (average of 720, $n = 15$), than in the carbonate stream (50 to 1150 ppmv, average of 357). DO was mostly supersaturated with respect to atmo-spheric O_2, showing average DO_{sat} of 1.21 and 1.22 in the streams in the silicate and carbonate catchments, respectively.
15   Alkalinity was the parameter that differentiated stream waters (Fig. 3). Both stream waters had higher pH than the respective spring water in each catchment. Compared with the respective spring water, alkalinity was higher in the silicate stream, but was lower in the carbonate stream.

4 Discussion

20 ### 4.1 Sources of spring water DIC

The clear distinction in geochemical and carbon isotope characteristics between the two spring waters indicated that the springs may have retained pristine characteristics of the groundwater in each catchment. To examine this, we calculated expected carbon isotopic composition of groundwater DIC originating exclusively from soil CO_2 (silicate
25 catchment) and from a 1:1 mixture of soil CO_2 and carbonate minerals (carbonate

catchment) (Clark and Fritz, 1997). We assumed that soil organic matter was from C3 plants with a mean $\delta^{13}C$ of −27‰ (O'Leary, 1988) and used the temperature dependence of carbon isotope fractionation between CO_2 and H_2CO_3/HCO_3^- (Zhang et al., 1995). The ratio between H_2CO_3 and HCO_3^- was calculated using K_1/a^{H^+}, where K_1 is the first dissociation constant of H_2CO_3, and a^{H^+} was calculated from the measured pH. The expected average $\delta^{13}C_{DIC}$ in the silicate spring (with 35% HCO_3^- and 65% H_2CO_3 at the average pH of 6.1) derived from soil CO_2 was −24.7‰, which was significantly lower than the measured average value of −16.2 ± 2.7‰. For the carbonate spring, the expected $\delta^{13}C_{DIC}$ (over 99.9% HCO_3^- at the average pH of 8.0) derived from 1:1 mixture of soil CO_2 and carbonate minerals was −9.0‰, which was close to the measured average value (−9.7 ± 1.5‰).

The discrepancy between measured and expected $\delta^{13}C_{DIC}$ values may be related to the presence of C4 plants (mostly corn) in the catchment area and/or degassing of CO_2 during the residence of water in the soil and groundwater reservoirs. The effect of C4 plant material cannot be quantitatively examined due to the lack of carbon isotope data of soil organic matter. The second possibility can explain the greater discrepancy observed in the silicate catchment. Because the proportion of dissolved CO_2 (H_2CO_3) in the total DIC was large in the silicate spring due to relatively low pH, the effect of CO_2 degassing was more significant. This interpretation is validated by the negative correlation ($r^2 = 0.92$) between pCO_2 and $\delta^{13}C_{DIC}$ and by the fact that water samples with higher pCO_2 showed $\delta^{13}C_{DIC}$ values closer to those of expected groundwater DIC (Fig. 4a). To verify the effect of CO_2 degassing on $\delta^{13}C_{DIC}$ of the silicate spring, we referred to the study by Doctor et al. (2007). They reported that the increase in $\delta^{13}C_{DIC}$ per natural log-unit decrease of excess pCO_2 was 2.4‰, where excess pCO_2 is the measured pCO_2 normalized to the expected pCO_2 at atmospheric equilibrium. In our study, the relationship was calculated as a 2.3 ± 0.2‰ increase per unit decrease of excess pCO_2, indicating that the variability in silicate spring $\delta^{13}C_{DIC}$ closely followed the reported change associated with the CO_2 degassing. DIC in the carbonate spring

Dissolved inorganic carbon export from carbonate and silicate

W. J. Shin et al.

Title Page

Abstract | Introduction

Conclusions | References

Tables | Figures

|◄ | ►|

◄ | ►

Back | Close

Full Screen / Esc

Printer-friendly Version

Interactive Discussion

water consisted primarily of HCO_3^-; therefore, the effect of CO_2 degassing and associated enrichment of ^{13}C was not as remarkable as were those effects in the silicate spring. In summary, the spring waters may well represent the groundwater component modified by the CO_2 degassing to a variable degree.

4.2 The evolution of $\delta^{13}C_{DIC}$ in stream waters

Because the spring waters likely represent the source groundwater composition, it is informative to compare spring and stream waters to understand processes occurring along the hydrological pathways. Although the variability in $\delta^{13}C_{DIC}$ values between stream and spring waters was generally correlated in each catchment (with $r^2 = 0.62$ in the carbonate and $r^2 = 0.31$ in the silicate catchment), the difference between catchments was reduced (~0.9‰ between streams compared to ~6.5‰ between springs) and DIC was more enriched in ^{13}C in stream waters. The increase in $\delta^{13}C_{DIC}$ was likely related to aquatic photosynthesis and CO_2 degassing.

To examine the relative importance of aquatic photosynthesis and CO_2 degassing, we plotted the difference in $\delta^{13}C_{DIC}$ between the spring and stream waters ($\Delta\delta^{13}C_{DIC}$) against the dissolved O_2 saturation (DO_{sat}) in stream waters (Fig. 5a) and the difference in pCO_2 between the spring and stream waters (ΔpCO_2) (Fig. 5b). Because the stream waters were mostly over-saturated with O_2 relative to atmospheric equilibrium, photosynthesis was assumed to be prevalent, and associated ^{13}C enrichment was expected. However, the correlation between $\Delta\delta^{13}C_{DIC}$ and DO_{sat} was low ($r^2 < 0.1$), indicating that aquatic photosynthesis may not have been the major process for ^{13}C enrichment. In addition, if photosynthesis resulted in ^{13}C enrichment, there would have been a seasonal difference in $\delta^{13}C_{DIC}$ because photosynthesis is more intense in summer than in winter. However, the magnitude of ^{13}C enrichment was similar regardless of the season.

In contrast, $\Delta\delta^{13}C_{DIC}$ exhibited a higher correlation ($r^2 = 0.52$ and 0.43) with ΔpCO_2 in both catchments. Therefore, a simplified interpretation regarding the enrichment of

^{13}C in stream water DIC is that it was caused mainly due to CO_2 degassing along the pathways from the groundwater reservoirs to the stream. In the carbonate catchment, $\Delta\delta^{13}C_{DIC}$ was comparatively small because of the minor proportion of dissolved CO_2 (<0.1%) in the total DIC; thus, the effect of CO_2 degassing from the groundwater was smaller than that in the silicate catchment. Moreover, due to the slight under-saturation with CO_2 in the carbonate stream, CO_2 dissolution may also have occurred that led to a different degree of ^{13}C enrichment compared to that expected from CO_2 degassing.

4.3 Seasonal variation in $\delta^{13}C_{DIC}$ and carbonate chemistry

The spring and stream samples exhibited well-defined seasonal variations characterized by low $\delta^{13}C_{DIC}$ values during summer (June to September) and high $\delta^{13}C_{DIC}$ values during winter (November to February) (Fig. 2b). In addition, pCO_2 showed a seasonal dependence, with higher values during June–October and lower values during November–March, especially in the silicate spring water (Fig. 2c). In the study area, the observed seasonality could have been due to (1) the seasonal change in metabolic activity related to changes in temperature and (2) changes in the water regime related to precipitation patterns.

Because both stream waters were assumed to be dominantly photosynthetic, the higher pCO_2 during summer does not support in-situ production, but likely reflects CO_2 transport from soils via groundwater discharge associated with the enhanced microbial and root respiration during the season (Barth and Veizer, 1999; Hamada and Tanaka, 2001; Hope et al., 2004; Xie et al., 2005; Yao et al., 2007; Jin et al., 2008). The addition of soil CO_2 via soil/groundwater resulted in low $\delta^{13}C_{DIC}$ values of the water. A negative correlation between $\delta^{13}C_{DIC}$ and pCO_2 in the spring samples in the silicate catchment indicates that soil-derived CO_2 was the main cause of seasonality in $\delta^{13}C_{DIC}$ values (Fig. 4a). The correlation between $\delta^{13}C_{DIC}$ and pCO_2 in other types of water was not as obvious as in the spring samples in the silicate catchment. In the carbonate catchment, the changes in $\delta^{13}C_{DIC}$ were positively correlated with EC

in the spring ($r^2 = 0.58$) and stream ($r^2 = 0.49$) waters (Fig. 4b), and waters with low EC occurred during the summer when $\delta^{13}C_{DIC}$ values were also low. EC increased as the residence time of water in soil and groundwater reservoirs increased; thus, during summer, EC decreased due to the higher precipitation and rapid turnover of subsur-
5 face water (Clark and Fritz, 1997). This indicates that the seasonality of $\delta^{13}C_{DIC}$ in the carbonate catchment was related to the change of the water regime due to seasonal precipitation patterns.

Precipitation, which was measured at the Yeongweol meteorological station about 40 km from the study area (data from Korea Meteorological Administration, KMA:
10 www.kma.go.kr), varied throughout the study period (Fig. 2a). The average monthly precipitation during summer and early fall (June to October) was 202.8 mm, but for the rest of the year (November to May) it was only 39.3 mm. The seasonal variation of precipitation roughly coincided with the fluctuations in $\delta^{13}C_{DIC}$ (Fig. 2b) of all water samples and in EC (Fig. 4b) of the carbonate catchment. During the dry season
15 (October to May), pore water has a long residence time in the soil horizon, allowing for an extended exchange of CO_2 with the atmosphere through the soil zone, thereby increasing $\delta^{13}C_{DIC}$ and EC of the soil water. In contrast, during the wet season (June to September), the frequent infiltration of rainwater into the soil and the outflow of interstitial soil waters from the vadose zone result in a shorter residence time for soil
20 water and limit CO_2 exchange with the atmosphere. Therefore, soil water in summer and early fall displays lower $\delta^{13}C_{DIC}$ values and EC than does soil water during the winter season (Amiotte-Suchet et al., 1999). The transport of CO_2 produced by soil respiration via soil/groundwaters with distinct EC is facilitated by the concentrated precipitation in summer. The effect of pCO_2 was not clearly observed in the waters from
25 the carbonate catchment due to lower CO_2/HCO_3^- ratios, but the analogous effect associated with seasonal changes in soil respiration and water regime can be expressed by EC vs. $\delta^{13}C_{DIC}$ plots (Fig. 4b).

4.4 DIC export from the river system

The importance of CO_2 degassing was suggested from the previous discussion on the changes in $\delta^{13}C_{DIC}$ values of spring and stream waters. The calculated excess pCO_2 was 19.8 in the silicate spring, 3.3 in the carbonate spring, 1.9 in the silicate stream, and 0.9 in the carbonate stream (all as annual averages in 2005). Except for the carbonate stream, the studied waters were over-saturated with CO_2 and assumed to act as the source of atmospheric CO_2 (Yao et al., 2007). Although the excess pCO_2 in the carbonate stream was lower than 1, indicating possible invasion of atmospheric CO_2, its DIC was still depleted in ^{13}C compared with atmosphere-derived DIC ($\sim$0‰, assuming $\delta^{13}C$ of atmospheric CO_2 to be -7.8‰ from Brunet et al., 2005).

To quantitatively determine the amount of CO_2 degassing, we applied the following flux equation:

$$F = k_{CO_2}(C_{eq} - C),$$

where F is the diffusive flux of CO_2 to the atmosphere, k_{CO_2} is the gas transfer coefficient, and C_{eq} and C are the dissolved CO_2 concentrations in equilibrium with the atmosphere and as measured, respectively. Because k_{CO_2} was not determined in this study, we calculated F for all possible ranges of k_{CO_2} using various relationships between wind speed and k_{CO_2}. The estimated k_{CO_2} ranged from 0.14 m d^{-1} (based on Wanninkhof, 1992) to 1.92 m d^{-1} (based on Borges et al., 2004) at the mean wind speed of 1.54 m s^{-1} during the study period (from KMA). The carbon flux to the atmosphere was estimated at 220 to 3000 g C m^{-2} y^{-1} for the silicate spring water and 30 to 430 g C m^{-2} y^{-1} for the carbonate spring water. The silicate stream water had a carbon flux of 10 to 150 g C m^{-2} y^{-1}, whereas the carbonate stream water may have incorporated atmospheric CO_2 at rates of 2 to 30 g C m^{-2} y^{-1}. Although the estimated carbon flux was within the range reported in other studies (Richey et al., 2002; Yao et al., 2007; Brunet et al., 2009; Dubois et al., 2010), it is notable that the effect varied depending on the catchment lithology. In terms of the atmospheric CO_2 budget,

the silicate catchments were assumed to act as stronger sources than the carbonate catchments, and carbonate stream waters may even act as a minor sink.

Table 3 presents a comprehensive carbon budget for the studied river systems. A few assumptions were made to derive the catchment-scale carbon budget. First, the data measured at the mouth of the stream collectively represent the carbon exchange characteristics of the stream waters, except for the first-order streams in the catchment. The first-order streams likely retained characteristics of the groundwater, which diminish in the higher-order streams (Johnson et al., 2008). Second, the spring waters represent the subsurface waters in each catchment, as discussed in Sect. 4.1. Third, the stream waters consisted primarily of discharged groundwater, although the hydrograph separation of the studied streams was not available.

The DIC discharge via the stream was the largest component, ranging from 12.7 $\mathrm{g\,C\,m^{-2}\,y^{-1}}$ in the silicate catchment to 38.3 $\mathrm{g\,C\,m^{-2}\,y^{-1}}$ in the carbonate catchment (data are normalized to the catchment area). CO_2 degassing from the stream (higher than second order) was 0.05 to 0.68 $\mathrm{g\,C\,m^{-2}\,y^{-1}}$ in the silicate catchment, whereas CO_2 dissolution of –0.01 to –0.17 $\mathrm{g\,C\,m^{-2}\,y^{-1}}$ occurred in the carbonate stream. Notably, the estimated CO_2 degassing associated with the groundwater discharge was significant, 1.1 to 14.9 $\mathrm{g\,C\,m^{-2}\,y^{-1}}$ in the silicate catchment and 0.17 to 2.4 $\mathrm{g\,C\,m^{-2}\,y^{-1}}$ in the carbonate catchment. Depending on the adopted k_{CO_2}, the CO_2 degassing (from both stream and groundwater) may have been responsible for 8–55% of the total DIC export from the silicate catchment, whereas it took up only 0.4–5.6% in the carbonate catchment. The results clearly indicate that CO_2 degassing at the interface between groundwater and streams in headwater regions needs to be considered to derive a reliable carbon budget in river systems, especially in silicate-dominant catchments.

Our carbon budget estimates are different from those in other studies because we considered the CO_2 degassing during groundwater discharge into the stream. However, uncertainties may exist in our estimation of CO_2 evasion from groundwater. For example, there is uncertainty related to the characterization of the interface between

groundwater and the stream because the quantity of CO_2 degassing depends on the dimension of the water surface. We assumed that the interface was the first-order stream where the immediate confluence of groundwater occurs. Previous studies (Johnson et al., 2008; Öquist et al., 2009) reported that the evasion of CO_2, accompanied by

5   subsurface water input, was concentrated along a short distance ($\sim$200 m) of stream water from the confluence, which may substantiate our assumption. Another uncertainty is related to the proportion of groundwater components in the stream. Stream waters may contain variable amounts of surface runoff and direct precipitation. Hydrograph separation using various tracers can give quantitative estimates of these water

10   components (Genereaux and Hooper, 1998). Because we assumed that the stream water was mostly derived from groundwater, the CO_2 degassing estimates in this study likely represent the highest possible amount.

5   Conclusions

The uppermost tributaries of the SHR, South Korea, provided an ideal natural setting to

15   examine the effects of catchment lithology, seasonality in metabolic activities and water regimes, and atmospheric exchange on $\delta^{13}C_{DIC}$ values and carbonate chemistry. The relatively pristine DIC sources can be represented by spring waters, which clearly exhibited the effects of catchment lithology, i.e., silicate vs. carbonate, on $\delta^{13}C_{DIC}$ values. Seasonal variations were obvious in relation to the temperature-induced changes

20   in metabolic activities and the precipitation-induced changes in hydrologic regimes. Both stream waters were enriched with ^{13}C compared to the respective spring waters. This was in part due to aquatic photosynthesis, but was primarily caused by CO_2 degassing, which occurred from the groundwater and streams, but the magnitude was far greater from the groundwater. The estimated carbon budget depended on

25   the catchment lithology. In the silicate catchment, CO_2 degassing associated with the groundwater discharge could be as high as the DIC discharge via the rivers. In contrast, DIC discharge via stream waters far exceeded CO_2 degassing from groundwater

in the carbonate catchment, with possible CO_2 uptake by the stream. We emphasize the importance of CO_2 export associated with groundwater discharge at the headwater regions and its variability with the catchment lithology for a more comprehensive carbon budget of river systems.

References

Acour, A. M., Sheppard, S. M. F., Guyomar, O., and Wattelet, J.: Use of ^{13}C to trace origin and cycling of inorganic carbon in the Rhone River system, Chem. Geol., 159, 87–105. 1999.

Amiotte-Suchet, P., Aubert, D., Probst, J. L., Gauthier-Lafaye, F., Probst, A., Andreux, F., and Viville, D.: δ^{13}C pattern of dissolved inorganic carbon in a small granitic catchment: the Strengbach case study (Vosges Mountains, France), Chem. Geol., 159, 129–145, 1999.

Atekwana, E. A. and Krishnamurthy, R. V.: Seasonal variations of dissolved inorganic carbon and δ^{13}C of surface waters: application of a modified gas evolution technique, J. Hydrol., 205, 265–278, 1998.

Barth, J. A. C. and Veizer, J.: Carbon cycle in St. Lawrence aquatic ecosystems at Cornwall (Ontario), Canada: seasonal and spatial variations, Chem. Geol., 159, 107–128, 1999.

Borges, A. V., Vanderborght, J.-P., Schiettecatte, L.-S., Gazeau, F., Ferrón-Smith, S., Delille, B., and Frankignoulle, M.: Variability of the gas transfer velocity of CO_2 in a macrotidal estuary (the Scheldt), Estuaries, 27, 593–603, doi:10.1007/BF02907647, 2004.

Brunet, F., Gaiero, D., Probst, J. L., Depetris, P. J., Gauthier Lafaye, F., and Stille, P.: δ^{13}C tracing of dissolved inorganic carbon sources in Patagonian rivers (Argentina), Hydrol. Process., 19, 3321–3344, 2005.

Brunet, F., Dubois, K., Veizer, J., Nkoue Ndondo, G. R., Nadam Ngoupayou, J. R., Boeglin, J. L.,

Title Page

Abstract | Introduction

Conclusions | References

Tables | Figures

◄ | ►|

◄ | ►

Back | Close

Full Screen / Esc

Printer-friendly Version

Interactive Discussion

and Probst, J. L.: Terrestrial and fluvial carbon fluxes in a tropical watershed: Nyong Basin, Cameroon, Chem. Geol., 265, 563–572, 2009.

Clark, I. D. and Fritz, P.: Environmental Isotope Hydrogeology, Lewis Publishers, New York, 1997.

Dubois, K. D., Lee, D., and Veizer, J.: Isotopic constraints on alkalinity, dissolved organic carbon, and atmospheric carbon dioxide fluxes in the Mississippi River, J. Geophys. Res., 115, G02018, doi:10.1029/2009JG001102, 2010.

Finlay, J. C.: Controls of streamwater dissolved inorganic carbon dynamics in a forested watreshed, Biogeochemistry, 62, 231–252, 2003.

Friedlingstein, P., Dufresne, J.-L., Cox, P. M., and Rayner, P.: How positive is the feedback between climate change and the carbon cycle?, Tellus, 55B, 692–700, 2003.

Genereux, D. P. and Hooper, R. P.: Oxygen and hydrogen isotopes in rainfall-runoff studies, in: Isotope Tracers in Catchment Hydrology, edited by: Kendall, C. and McDonell, J. J., Elsevier, Amsterdam, 319–346, 1998.

Govindasamy, B., Thompson, S., Mirin, A., Wickett, M., Caldeira, K., and Delire, C.: Increase of carbon cycle feedback with climate sensitivity: results from a coupled climate and carbon cycle model, Tellus, 57B, 153–163, 2005.

Hélie, J. F., Haillaire-Marcel, C., and Rondeau, B.: Seasonal changes in the sources and fluxes of dissolved inorganic carbon through the St. Lawrence River – isotopic and chemical constraint, Chem. Geol., 186, 117–138, 2002.

Hamada, Y. and Tanaka, T.: Dynamics of carbon dioxide in soil profiles based on long-term field observation, Hydrol. Process., 15, 1829–1845, 2001.

Hope, D., Palmer, S. M., Billett, M. F., and Dawson, J. J. C.: Variations in dissolved CO_2 and CH_4 in a first-order stream and catchment: an investigation of soil-stream linkages, Hydrol. Process., 18, 3255–3275, 2004.

Jin, L., Williams, E. L., Szramek, K. J., Walter, L. M., and Hamilton, S. K.: Silicate and carbonate mineral weathering in soil profiles developed on Pleistocene glacial drift (Michigan, USA): mass balances on soil water geochemistry, Geochim. Cosmochim. Ac., 72, 1027–1042, 2008.

Johnson, M. S., Lehmann, J., Riha, S. J., Krusche, A. V., Richey, J. E., Ometto, J. P. H. B., and Couto, E. G.: CO_2 efflux from Amazonian headwater streams represents a significant fate for deep soil respiration, Geophys. Res. Lett., 35, L17401, doi:10.1029/2008GL034619, 2008.

Kim, J. C., Koh, H. J., Lee, S. R., Lee, C. B., Choi, S. J., and Park, K. H.: Geologic map and

Dissolved inorganic carbon export from carbonate and silicate

W. J. Shin et al.

Title Page

Abstract	Introduction
Conclusions	References
Tables	Figures

◄◄ ►►

◄ ►

Back Close

Full Screen / Esc

Printer-friendly Version

Interactive Discussion

explanatory note of the Gangreung-Sokcho sheet, Korea Institute of Geoscience and Mineral Resources, Daejeon, Korea, 2001.

Lee, K. S., Ryu, J. S., Ahn, K. H., Chang, H. W., and Lee, D.: Factors controlling carbon isotope ratios of dissolved inorganic carbon in two major tributaries of the Han River, Korea, Hydrol. Process., 21, 500–509, 2007.

Ludwig, W., Amiotte-Suchert, P., Munhoven, G., and Probst, J. L.: Atmospheric CO_2 consumption by continental erosion: present-day control and implications for the last glacial maximum, Global Planet. Change, 16–17, 107–120, 1997.

Meybeck, M.: Global chemical weathering of surficial rocks estimated from river dissolved loads, Am. J. Sci., 287, 401–428, 1987.

Mortatti, J. and Probst, J. L.: Silicate rock weathering and atmospheric/soil CO_2 uptake in the Amazon Basin estimated from river water geochemistry: seasonal and spatial variations, Chem. Geol., 197, 177–196, 2003.

O'Leary, M. H.: Carbon isotopes in photosynthesis, Bioscience, 38, 328–336, 1988.

Öquist, M. G., Wallin, M., Seibert, J., Bishop, K., and Laudon, H.: Dissolved inorganic carbon export across the soil/stream interface and its fate in a boreal headwater stream, Environ. Sci. Technol., 43, 7364–7369, 2009.

Parkhust, D. L. and Appelo, C. A. J.: User's guide to PHREEQC (version 2) – a computer program for speciation, batch-reaction, one-dimensional transport, and inverse geochemical calculations, US Geological Survey Water-Resources Investigations Report, USGS, 99–4259, 312 pp., 1999.

Raymond, P. A. and Bauer, J. E.: Atmospheric CO_2 evasion, dissolved inorganic carbon production, and net heterotrophy in the York River estuary, Limnol. Oceanogr., 45, 1707–1717, 2000.

Richey, J. E., Melack, J. M., Aufdenkampe, A. K., Ballester, V. M., and Hess, L. L.: Outgassing from Amazonian rivers and wetlands as a large tropical source of atmospheric CO_2, Nature, 416, 617–620, 2002.

Round, S. A. and Wilde, F. D.: Field Measurements: US Geological Survey Techniques of Water-Resources investigations, Book 9, Chapt. A6., Sect. 6.2, USGS, 2001.

Tan, F. C. and Edmond, J. M.: Carbon isotope geochemistry of the Orinoco Basin, Estuar. Coast. Shelf S., 36, 541–547, 1993.

Taylor, C. B. and Fox, V. J.: An isotopic study of dissolved inorganic carbon in the catchment of the Waimakariri River and deep ground water of the North Canterbury Plains, New Zealand,

Title Page

Abstract | Introduction

Conclusions | References

Tables | Figures

◀ | ▶

◀ | ▶

Back | Close

Full Screen / Esc

Printer-friendly Version

Interactive Discussion

J. Hydrol., 186, 161–190, 1996.

Telmer, K. and Veizer, J.: Carbon fluxes, pCO_2 and substrate weathering in a large northern river basin, Canada: carbon isotope perspectives, Chem. Geol., 159, 61–86, 1999.

Wang, X. and Veizer, J.: Respiration-photosynthesis balance of terrestrial aquatic ecosystem, Ottawa area, Canada, Geochim. Cosmochim. Ac., 64, 3775–3786, 2000.

Wanninkhof, R.: Relationship between wind speed and gas exchange over the ocean, J. Geophys. Res., 97, 7373–7382, doi:10.1029/92JC00188, 1992.

Xie, Z., Cadisch, G., Edwards, G., Baggs, E. M., and Blum, H.: Carbon dynamics in a temperate grassland soil after 9 years exposure to elevated CO_2 (Swiss FACE), Soil Biol. Biochem., 37, 1387–1395, 2005.

Yang, C., Telmer, K., and Veizer, J.: Chemical dynamics of the "St. Lawrence" riverine system: δD_{H_2O}, $\delta^{18}O_{H2_O}$, $\delta^{13}C_{DIC}$, $\delta^{34}S_{sulfate}$, and dissolved $^{87}Sr/^{86}Sr$, Geochim. Cosmochim. Ac., 60, 851–866, 1996.

Yao, G., Gao, Q., Wang, Z., Huang, X., He, T., Zhang, Y., Jiao, S., and Ding, J.: Dynamics of CO_2 partial pressure and CO_2 outgassing in the lower reaches of the Xijiang River, a subtropical monsoon river in China, Sci. Total Environ., 376, 255–266, 2007.

Zhang, J., Quay, O. D., and Wilbur, D. O.: Carbon isotope fractionation during gas-water exchange and dissolution of CO_2, Geochim. Cosmochim. Ac., 59, 107–114, 1995.

Dissolved inorganic carbon export from carbonate and silicate

W. J. Shin et al.

Title Page

Abstract	Introduction
Conclusions	References
Tables	Figures

|◄ | ►|

◄ | ►

Back | Close

Full Screen / Esc

Printer-friendly Version

Interactive Discussion

Table 1. Comparison of the physical characteristics and mean discharge for the Odae and Jijang catchments (Water Management Information System: www.wamis.go.kr).

Tributary	Odae (silicate)	Jijang (carbonate)
Catchment area (km^2)	452	225
Total stream length (km)	521	464
1st order stream length (km)	272	230
Main channel* length (km)	44	37
Mean width (m)	8.2	5.6
Mean discharge ($m^3\,s^{-1}$)	7	3

* Main channel corresponds to 5th order stream in both catchments.

Table 2. Statistical summary of geochemical parameters measured from springs and streams in the study area.

Parameters	Silicate catchment								Carbonate catchment							
	Spring water				Stream water				Spring water				Stream water			
	Min	Max	Aver	SD	Min	Max	Aver	SD	Min	Max	Aver	SD	Min	Max	Aver	SD
$\delta^{13}C_{DIC}$ (‰)	−21.2	−13.1	−16.2	2.7	−10.0	−3.6	−6.9	1.6	−13.2	−8.1	−9.7	1.5	−11.2	−6.1	−7.8	1.5
Temp. (°C)	8.8	12.7	10.7	1.3	0.4	28.0	11.0	8.9	8.9	14.3	11.6	1.9	0.3	28.0	13.0	8.4
pH	5.1	6.9	6.1	0.5	6.8	8.1	7.9	0.3	7.7	8.5	8.0	0.2	7.9	9.1	8.5	0.4
DO (mg L^{-1})	9.7	18.8	12.2	2.0	10.0	19.6	13.4	2.8	8.6	15.6	11.6	1.6	8.7	18.7	12.7	2.2
EC (μS cm^{-1})	ND	ND	ND	ND	11	122	64	31	171	389	254	62	222	433	301	60
Alk (meq L^{-1})	0.05	0.17	0.09	0.0	0.22	0.74	0.44	0.15	1.50	2.21	1.96	0.21	1.18	1.83	1.46	0.16
DIC (mg L^{-1})	5.6	103.3	22.7	23.3	13.7	45.5	26.0	10.0	93.1	137.9	121.8	12.8	71.3	110.2	91.0	12.0
pCO_2 (ppmv)	827	42 546	7520	10 239	150	3380	720	813y	372	2197	1245	466	50.3	1150	357	282

ND: not determined.
Min, Max, Aver, and SD represent minimum, maximum, average, and standard deviation, respectively.

Table 3. Estimated annual carbon budget of the studied catchments. All units are $g\,C\,m^2\,y^{-1}$ and normalized to the catchment area.

Tributary	Odae (silicate)	Jijang (carbonate)
DIC discharge via streams	12.7	38.3
CO_2 degassing from streams[*]	$0.05 \sim 0.68$	$-0.01 \sim -0.17$
CO_2 degassing from groundwater[*]	$1.1 \sim 14.9$	$0.17 \sim 2.4$

[*] Fluxes were calculated for the range of gas transfer coefficient.
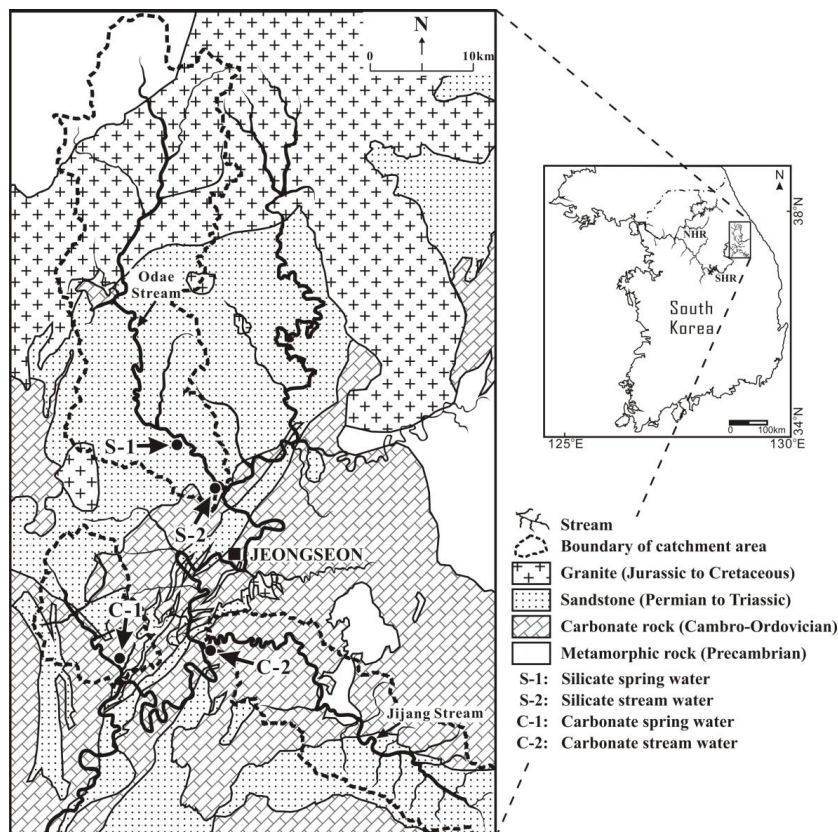
Fig. 1. Map showing the basement lithology and sampling locations of the studied catchments, two uppermost tributaries of the South Han River. Spring and stream waters in the silicate catchment were collected at S-1 and S-2, respectively; spring and stream waters in the carbonate catchment were collected at C-1 and C-2. NHR and SHR represent the North Han River and the South Han River, respectively.
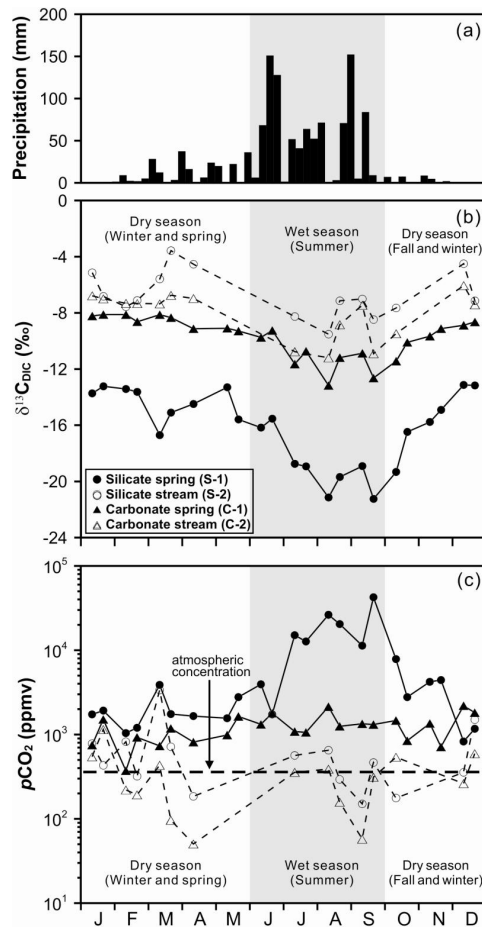
Fig. 2. Amount of precipitation **(a)**, $\delta^{13}C_{DIC}$ values **(b)**, and pCO_2 **(c)** of waters from the silicate and carbonate catchments during 2005.

Title Page

Abstract | Introduction

Conclusions | References

Tables | Figures

|◀ | ▶|

◀ | ▶

Back | Close

Full Screen / Esc

Printer-friendly Version

Interactive Discussion
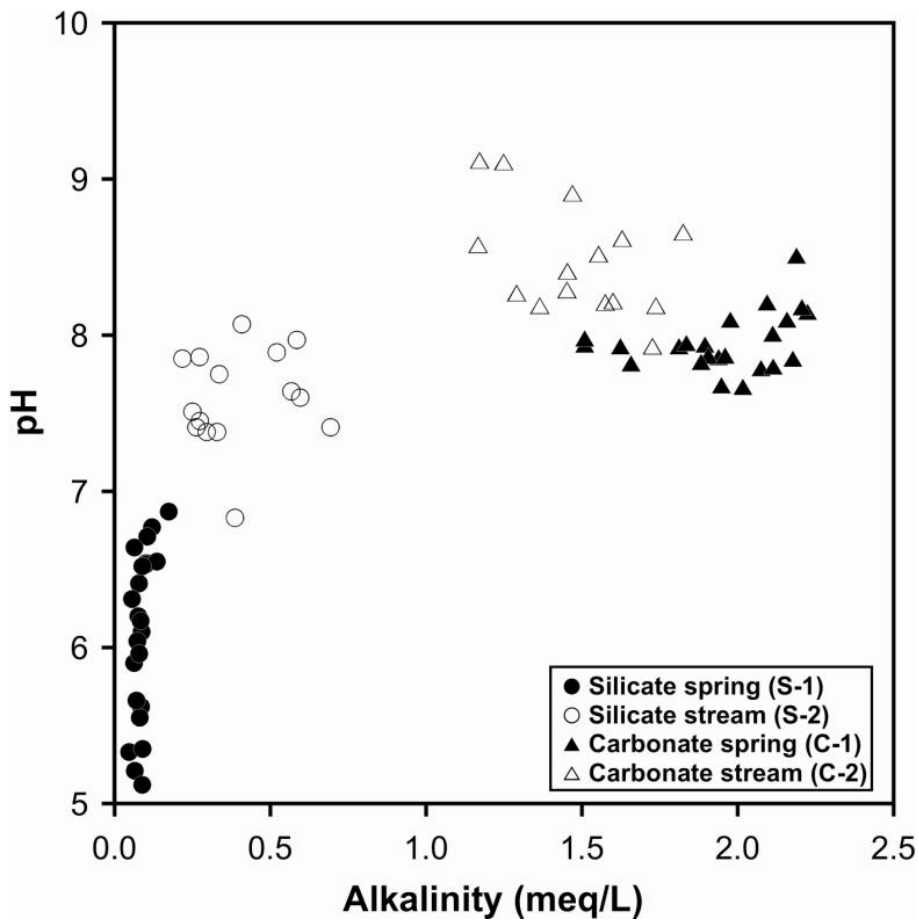
Fig. 3. Cross plot of alkalinity vs. pH in spring and stream waters. Note that the four different types of water are clearly distinguished in this figure.

Title Page

Abstract | Introduction

Conclusions | References

Tables | Figures

|◄ | ►|

◄ | ►

Back | Close

Full Screen / Esc

Printer-friendly Version

Interactive Discussion
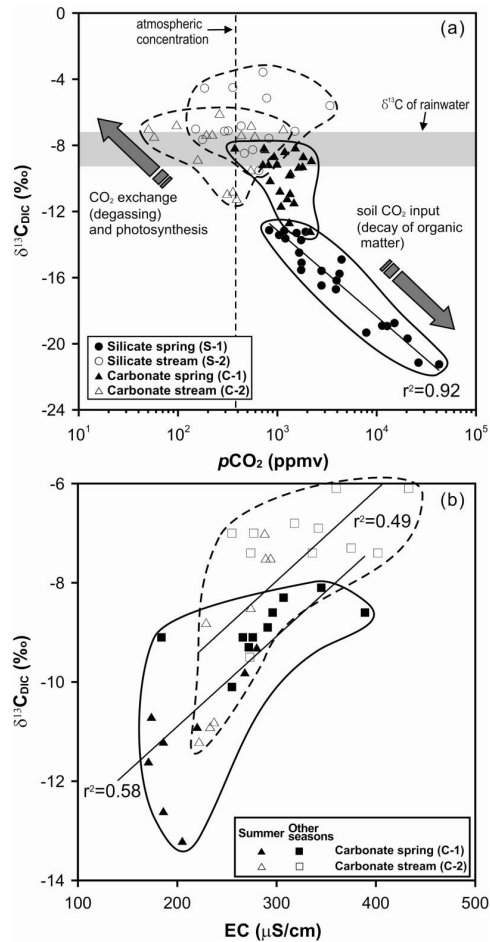
Fig. 4. Cross plots of pCO_2 vs. $\delta^{13}C_{DIC}$ **(a)**, and EC vs. $\delta^{13}C_{DIC}$ **(b)**. Summer = June through September. The $\delta^{13}C_{DIC}$ value of rainwater is from Zhang et al. (1995).

Title Page

Abstract | Introduction

Conclusions | References

Tables | Figures

◄ | ►►|

◄ | ►

Back | Close

Full Screen / Esc

Printer-friendly Version

Interactive Discussion
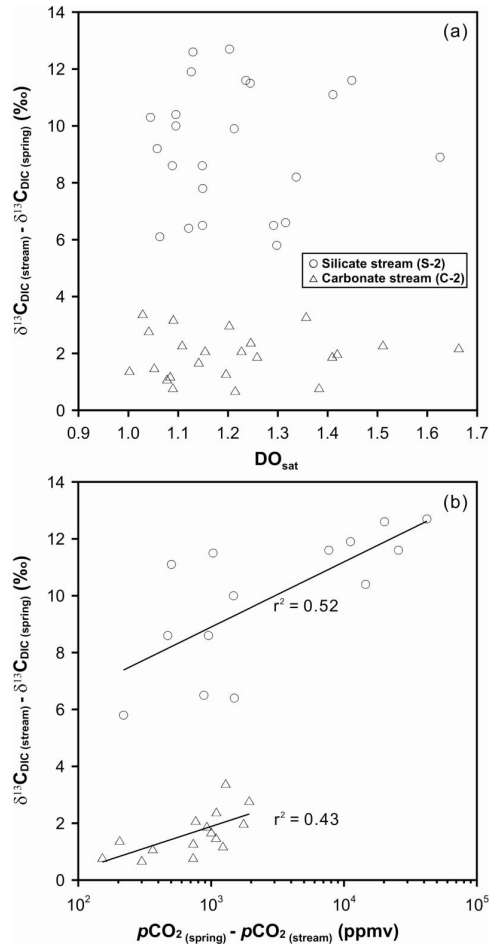
Fig. 5. Cross plots of **(a)** DO_{sat} vs. $\Delta\delta^{13}C_{DIC}$ [$\delta^{13}C_{DIC}$ (stream water) $-$ $\delta^{13}C_{DIC}$ (spring water)], and **(b)** ΔpCO_2 [pCO_2 (spring water) $-$ pCO_2 (stream water)] vs. $\Delta\delta^{13}C_{DIC}$.